

POLYGONAL NETWORKS RESULTING FROM DEWETTING

U. THIELE, M. MERTIG AND W. POMPE

*Institut für Werkstoffwissenschaft, TU Dresden,
Hallwachsstr. 3, D-01069 Dresden, Germany*

AND

H. WENDROCK

*Institut für Festkörper- und Werkstofforschung Dresden,
P.O.Box 16, D-01171 Dresden, Germany*

The occurrence of polygonal structures is widespread in nature [1]. Extensive investigations on the statistics of two-dimensional networks have been performed for biological tissues [2, 3], clusters of metal grains [4, 5], systems of soap bubbles [6, 7, 8], emulsion lattices [9], gas bubbles in Langmuir monolayers [10], magnetic froth [11] or convective patterns in hydrodynamics [12, 13, 14]. The strong similarity between structure and evolution of two-dimensional soap froth and grain boundary networks has become a subject of growing interest [15, 16, 17, 6]. These similarities make it difficult to differentiate the networks occurring in different experimental systems. Additionally, one faces a problem if the system is two-dimensional because it is a planar cut of a three-dimensional systems (grain boundary network) or through putting the three-dimensional structure between two narrowly spaced glass plates (soap froth, emulsion lattice, magnetic froth). Here, we will introduce two new experimental systems representing dewetting processes of a thin liquid films on a solid substrates. The occurring polygonal networks are intrinsically two-dimensional. After a short introduction of the concepts of wetting and dewetting, the dewetting experiments of polystyrene on silicon and of collagen solution on highly oriented polygraphite are explained. The different stages of the dewetting process will be discussed at these examples. Main features of the resulting structures are analysed by means of stochastic geometry of polygonal networks. The resulting distributions are compared with distributions obtained for two-dimensional soap froth. Typical differences between dewetting patterns and soap froth and between the two dewetting patterns are explained by distinct driving forces behind structure formation.

Putting a macroscopic drop of liquid on a surface one can observe two different scenarios. Macroscopic means here bigger than the range of long range molecular interactions like Van-der-Waals forces but small enough that effects of gravity need not be taken into account¹. The drop of liquid can spread until a thin film covers the whole surface. The liquid wets the surface. The case is called complete wetting. On the other hand the drop can remain as a small spherical cap. The liquid does not wet the surface. This case is called partial wetting.

In both cases the driving force is the minimization of surface energy. The final state is characterized by the equilibrium contact angle θ_E between the liquid–gas and the liquid–substrate interface at the three-phase contact line. It can be calculated from the surface tensions with the help of the Youngs–relation:

$$\gamma_{SG} = \gamma_{SL} + \gamma_{LG} \cos \theta_E \quad (1)$$

where γ_{SG} , γ_{SL} and γ_{LG} denote the surface tensions of the solid–gas, solid–liquid and liquid–gas interface respectively. For $\gamma_{SG} - \gamma_{SL} > \gamma_{LG}$ the liquid wets the substrat.

Now, consider the situation, where a thin film of fluid is placed on the surface. This may be realized by spin-casting, floating or painting. What will happen? If the liquid wets the substrate the film remains. But taking a liquid that does not wet the substrate the film tries to reach its equilibrium configuration, i.e. it tries to form a single drop. A thicker film will retract at the borders in order to reach this state. If, however, the film is very thin (when it is brought onto the substrate by spin casting at high frequencies), it does not only draw back at the borders but also breaks up at many locations 'within' the film. In the course of this process, inner edges appear that also draw back. Or in other words, holes appear that grow with time. This process is called dewetting. We will discuss here patterns resulting from this process. (For an introduction into the subject see [18, 19, 20].)

Before the stages of the process are explained in more detail, the experimental systems are shortly introduced. Experiments on polystyrene (PS) films on silicon are described in [21, 22]. Thin films (thickness 20-300nm) are produced at room temperature by spin casting a solution of PS in toluen onto the silicon. Toluene evaporates and a smooth thin film of glassy PS is formed. When one brings the sample above the glass transition temperature, PS becomes a liquid at once and dewets from silicon. The process is observed time resolved with an optical microscope. All holes arise at nearly the same time at random distributed spots on the substrate[22]. The mechanism of formation of initial holes is still controversial. It may be a spontaneous instability of the thin film under the influence of long

¹The latter is the case for drops smaller than the capillary length.

range molecular forces [21, 23], or heterogeneous nucleation caused by defects [22, 24]. In the next stage of the process the holes grow till they meet each other. At first, neighbouring holes touch leaving a thin liquid bridge inbetween. The liquid bridge between the holes can either rupture, leading to hole coalescence, or remain stable. If the bridge remains stable, a thin rim of liquid is formed between the holes. The rims form the edges of a two-dimensional polygonal network resembling at the first sight to a two-dimensional aged soap froth. The diameters of the polygonal cells are in the range of $10\text{-}100\mu\text{m}$ (see Fig.1d).

But this is only a transient state. On a longer timescale the liquid rims are not stable. They may decay into rows of drops via a Rayleigh instability.

We have investigated acedic collagen solution (CS) that is spin-casted on highly oriented polygraphite (HOPG) [25]. After the deposition of the film (thickness $10\text{-}15\mu\text{m}$) the solvent begins to evaporate. Evaporation continues during all the process. In competition with evaporation, hole nucleation sets in. The holes grow, meet and form a polygonal network as in the PS experiment. But in contrast with PS films, the nucleation of holes continues during all stages of the process. The evolution of the structure only stops when all the solvent is evaporated. The pattern resulting from dewetting is fixed in the dried collagen and can be imaged by scanning force microscopy (cell diameter below $1\mu\text{m}$). The rate of evaporation and therefore the observed stage of the dewetting process can be controlled by humidity. In Fig.1a-c three stages of this process are shown. In order to get this series of images, different collagen concentrations and different humidities are used. The edges of the polygonal network are stable, because they have approximatively the same size as the collagen molecules (relatively rigid rods of 300nm length). Thus coalescence of holes and the evolution of the rims into drops are suppressed. At this point it should be mentioned that both systems can show a dynamical instability of the moving liquid rim during hole growth: Liquid rims may lag behind the moving circular rim (so called back-fingering). In the case of the CS, this gives a transition between network-like pattern and tree-like patterns. Here, we restrict our attention to networks.

In order to characterize the network structures that form an intermediate state of the PS film and the final state for the collagen film evolution, we use methods of stochastic geometry of polygonal networks (SGPN) which are part of stochastic geometry. These methods were used extensively to analyse the evolution of 2d soap froths. They allow comparison between soap froth and dewetting structures. We are investigating the statistical distributions of network variables, such as number of edges, edge length, cell area, cell perimeter or angles between the edges. The mean values and second moments of these distributions give a first characterisation of the

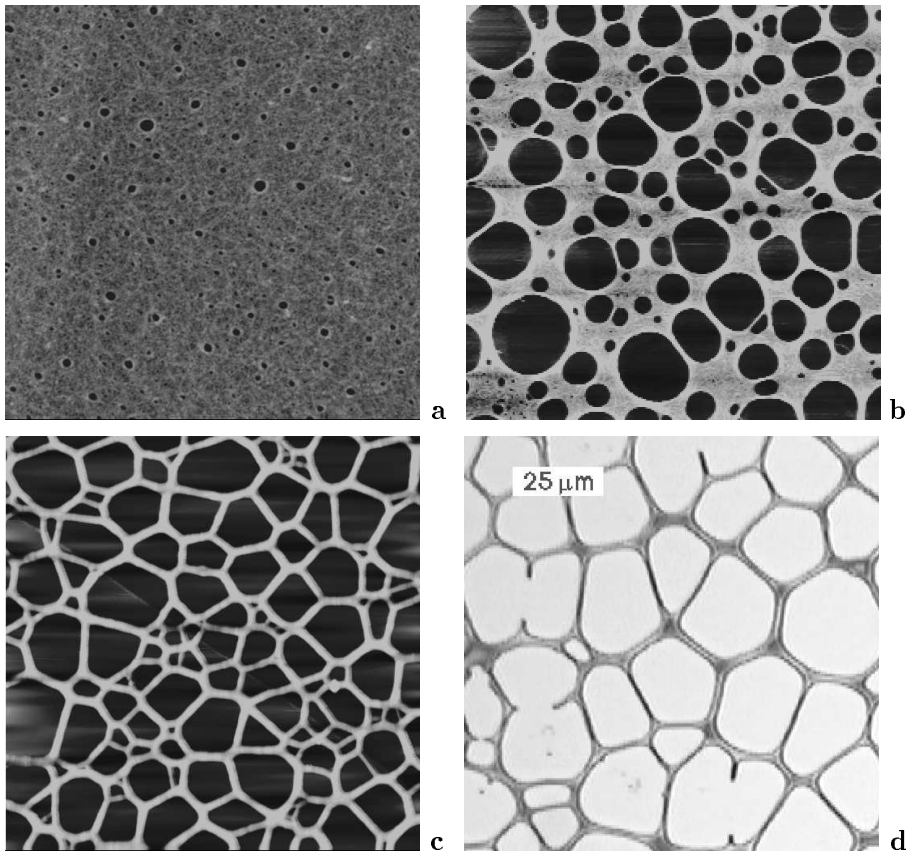


Figure 1. Structures obtained by dewetting for two different experimental systems: collagen solution on highly oriented polygraphite (a-c), and polystyrene on silicon [26] (d). For the collagen solution three stages of the evolution of holes are illustrated by final images taken at different experimental conditions. The images a-c show an area of 5 micron x 5 micron. (a) The formation of holes just started. (b) Intermediate state during hole growth. Some holes have touched. (c) Developed polygonal network, final state of the dewetting process of collagen films. (d) Developed polygonal network for PS on silicon. Some rims are ruptured, leading to coalescence of pores.

structures. One can further take into account correlations between neighbouring cells (for edge numbers: Aboav-Weaire law) or between different variables like for example cell area and edge number (Lewis law). Here we are interested in the distribution functions of the single variables only.

Fig.2a-d show the distributions of edge number, edge angle, cell perimeter and cell area. We show data from two samples of aged soap froth, dewetting network of PS films and of collagen films [27].

With respect to the edge angles we have to remark that the data rep-

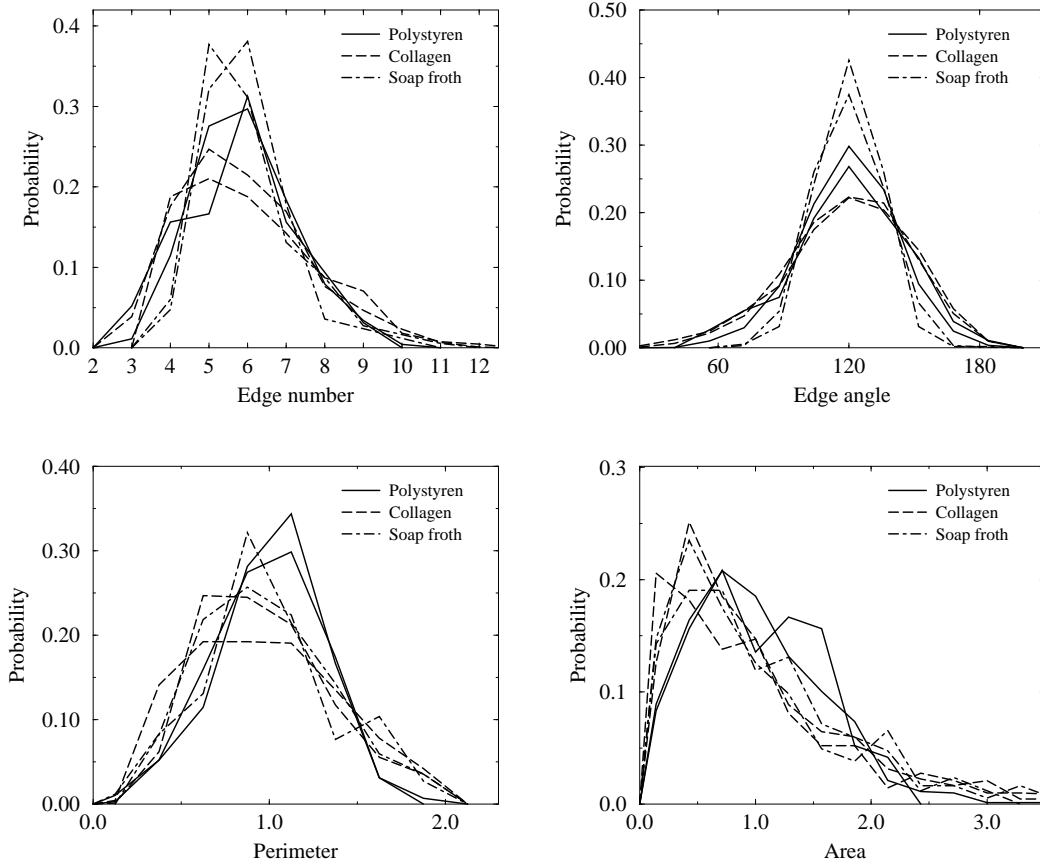


Figure 2. Comparison of distributions characterising the polygonal networks occurring in the dewetting process (polystyrene, collagen) and aged soap froth [27]. (a) Edge number distribution. (b) Distribution of angles between edges, where the straight lines between vertices are taken as edges. (c) Distribution of normalised cell perimeter. (d) Distribution of normalised cell area.

resent not the actual angles under which the edges meet locally at the vertices, but the angles that are given if one connects neighbouring vertices by straight lines (resulting from the image analysis procedure). This might be misleading if one wants to analyse the physics of a soap froth near the vertices however it gives nevertheless a good measure for comparison of different experimental systems as it is done here.

The distributions are in general quite similar for the same experimental system (meaning that they are reproducible), but show characteristic differences with respect to each other. Differences are more pronounced for

edge angle and edge number than for cell perimeter and area. To quantify these differences one has to study the characteristic variables of the distribution functions. Note first, that the mean values of the distributions are not relevant for a comparison. Networks with threefold vertices only have generally a mean value of the edge number $\langle n \rangle = 6$ and a mean value of the edge angle that is 120° . The mean value of the area gives only the length scale for the experimental system.

However as demonstrated in the following the normalised second moments are a good measure to compare networks resulting from different experimental systems. They are defined as follows:

$$\mu_2^f = \frac{1}{\langle f \rangle^2} \frac{1}{N} \sum_{i=1}^N (f_i - \langle f \rangle)^2, \quad (2)$$

where f denotes the relevant variable of the distribution (n edge number, p cell perimeter, a cell area and ω angle between edges), $\langle f \rangle$, its mean value, f_i , its value for cell i and N the number of cells. Normalisation of metric variables like perimeter and area is necessary in order to compare different networks. The normalisation is also used for the edge angles. The second moment of the edge number distribution μ_2^n is given without normalisation as in the literature. Higher moments are not discussed because of the restricted number of cells available for the statistical analysis. The second moments are listed in Tab.1. The second moment of the edge number dis-

TABLE 1. comparison of the second moments of collagen and polystyrene dewetting networks and soap froth

Property	Collagen	Polystyrene	Soap (aged)
μ_2^n	2 – 5	≈ 2	≈ 1.4
μ_2^a	0.4 – 1.5	≈ 0.3	0.4 – 1.2
μ_2^p	0.10 – 0.35	0.05-0.10	0.01 – 0.03
μ_2^ω	0.05 – 0.07	0.03 – 0.05	≈ 0.015

tribution μ_2^n that is usually taken as a measure of disorder indicates that dewetting structures are more disordered than soap froth. Among dewetting structures, PS patterns are more ordered than the collagen networks. This can be explained by coalescence of holes occurring during the evolution of the PS system. Coalescence happens through rupture of the thinnest rims, found mainly inbetween holes of very different sizes. Therefore, coalescence equilibrates the cell sizes. Indeed, μ_2^a is considerably smaller in PS than in CS.

By contrast, the evolution process of a soap froth is driven by pressure differences between neighbouring cells that are equilibrated by diffusion of gas through the cell walls. Cells with more than six sides grow at the expense of the cells with less than six sides that shrink (von Neumann's law) [15, 28]. Therefore, one finds always small and large cells, i.e. μ_2^a does not decrease in time in the steady state of an aged froth. Locally, the vertices stay in equilibrium; three edges meet at angles of 120° .

The evolution of soap froth and dewetting networks are therefore very different, as reflected by the second moments of the area distributions μ_2^a and the edge angle distribution μ_2^ω .

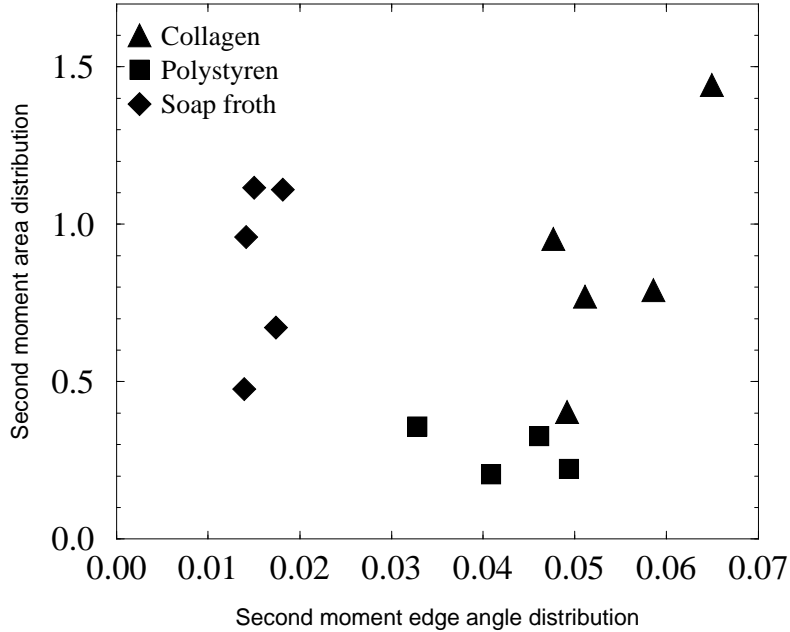


Figure 3. Shown is the second moment of the area distribution *vs.* the second moment of the distribution of edge angles for networks resulting from dewetting and two-dimensional soap froth respectively [29].

This is visualised in Fig.3 where μ_2^a is plotted over μ_2^ω . The dewetting pattern and the soap froth occupy different regions of the $\mu_2^\omega - \mu_2^a$ plane. Moreover dewetting patterns are clearly split into separate PS and CS regions. The soap froth has a very small μ_2^ω . We will call this vertex equilibrium. By contrast the PS pattern has a large μ_2^ω but a small μ_2^a . We call this edge equilibrium because the system tends to form edges that are stable on the time scale of the growth of the holes.

Because the collagen molecules suppress the coalescence of holes almost completely, the observed structures result from hole formation only. Neither edges nor vertices are in local equilibrium. This is reflected by the fact that both μ_2^a and μ_2^ω are large.

All the statistical distributions are a measure of the initial distribution of holes. Therefore they should resemble the distributions found for spatial tessellations generated with the Johnson-Mehl model [30, 31]. In this model one generates a random distribution of points (Poisson distribution). These points are activated at time t with a probability $p(t)$. Activated points grow into circular holes at constant velocity until they touch, ultimately filling the whole plane by a polygonal network. Let $p(t) \sim t^{(\beta-1)}$ be the probability of activating a point at time t . The exponent β can be negative or positive. For $\beta < 1$ the activation probability decreases with time, for $\beta > 1$ it increases whereas for $\beta = 1$ one gets a activation homogeneous in time. A delta function for $p(t)$ activates all points at once, and one obtains the Voronoi tessellation. This simultaneous activation can be ruled out, because the values of the second moments of a Voronoi tessellation are smaller than the collagen values (Voronoi: $\mu_2^n \approx 1.8$, $\mu_2^a \approx 0.3$, $\mu_2^p \approx 0.06$).

The evolution of the dewetting pattern itself suggests new extensions of the Johnson-Mehl model to interpret the experimental distributions. The standard Johnson-Mehl model can only be used for a qualitative comparison. For collagen films, it is not possible to extract a value for β by comparing model and experiment. The problem is that, experimentally, the rate of growth of the holes is not the same at all times. It decreases with increasing viscosity, as the solvent evaporates.

In conclusion dewetting of a thin liquid film is an interesting phenomena showing two-dimensional polygonal network formation. The direct comparison of networks of different physical origin with methods of stochastic geometry gives means to quantify the differences. It is possible to distinguish two local equilibriums: the vertex equilibrium of soap froth and the edge equilibrium of the coalescing dewetting network.

References

1. D. Weaire and N. Rivier. Soap, cells and statistics – Random patterns in two dimensions. *Contemp. Phys.*, 25(1):59–99, 1984.
2. F. T. Lewis. The geometry of growth and cell division in columnar parenchyma. *Am. J. Bot.*, 31:619–29, 1944.
3. J.C.M. Mombach, M.A.Z. Vasconcellos, and R.M.C. de Almeida. Arrangement of cells in vegetable tissues. *J. Phys. D*, 23(5):600–6, 1990.
4. D.A. Aboav. The arrangement of cells in a net. iv. *Metallography*, 18(2):129–47, 1985.
5. D.J. Srolovitz, M.P. Anderson, P.S. Sahni, and G.S. Grest. Computer simulation of grain growth. II. Grain size distribution, topology, and local dynamics. *Acta Met.*, 32(5):793–802, 1984.

6. J.A. Glazier, M.P. Anderson, and G.S. Grest. Coarsening in the two-dimensional soap froth and the large- q potts model: a detailed comparison. *Phil. Mag. B*, 62(6):615–45, 1990.
7. J. Stavans. The evolution of cellular structures. *Rep. Prog. Phys.*, 56(6):733–89, June 1993.
8. T. Aste, K. Y. Szeto, and W. Y. Tam. Statistical properties and shell analysis in random cellular structures. *Phys. Rev. E*, 54(4):5482–92, 1996.
9. D.A. Noever. Statistics of emulsion lattices. *Coll. Surf.*, 62(2):243, 1992.
10. B. Berge, A.J. Simon, and A. Libchaber. Dynamics of gas bubbles in monolayers. *Phys. Rev. A*, 41(12):6893–900, 1990.
11. F. Elias, C. Flament, J.-C. Bacri, and S. Neveu. Macro-organized patterns in ferrofluid layer: Experimental studies. *J. Phys. I France*, 7:711–28, 1997.
12. B. Simon and M. Belmedani. Cellular convection in shallow layers of aqueous solutions of sucrose: Lewis law. *C. R. Acad. Sci.*, 319(8):865–71, Oct. 1994.
13. P. Cerisier, S. Rahal, and N. Rivier. Topological correlations in benard-marangoni convective structures. *Phys. Rev. E*, 54(3):5086, 1996.
14. U. Thiele and K. Eckert. Stochastic geometry of polygonal networks – an alternative approach to the hexagon–square–transition in Bénard convection. *Preprint*, 1997.
15. C. S. Smith. *Metal Interfaces*, p. 65. American Society for Metals, Cleveland, Ohio, 1952.
16. D.A. Aboav. Foam and polycrystal. *Metallography*, 5:251–63, 1972.
17. M.A. Fortes and A.C. Ferro. Topology and transformations in cellular structures. *Acta Met.*, 33(9):1697–708, 1985.
18. P.G. de Gennes. Wetting: statistics and dynamics. *Rev. Mod. Phys.*, 57(3):827–63, 1985.
19. S. Dietrich. Wetting phenomena. *Phase Transitions and Critical Phenomena*, Vol. 12, p. 1. Academic Press, London, 1988.
20. F. Brochard-Wyart and J. Daillant. Drying of solids wetted by thin liquid films. *Can. J. Phys.*, 68(9):1084–8, 1989.
21. G. Reiter. Dewetting of thin polymer films. *Phys. Rev. Lett.*, 68(1):75–8, 1992.
22. K. Jacobs. *Stabilität und Dynamik flüssiger Polymerfilme*. Konstanz, 1997. Phd-thesis, ISBN 3-930803-10-0.
23. A. Sharma and G. Reiter. Instability of thin polymer films on coated substrates: Rupture, dewetting and drop formation. *J. Coll. Interf. Sci.*, 178:383, 1996.
24. K. Jacobs, S. Herminghaus, and G. Schatz. Dominance of defects in thin liquid polymer film rupture. *Preprint*, 1997.
25. M. Mertig, U. Thiele, J. Bradt, G. Leibiger, W. Pompe, and H. Wendrock. Scanning force microscopy and geometrical analysis of two-dimensional collagen network formation. *Surf. Int. Anal.*, 25:514–521, 1997.
26. PS: unpublished image by G. Reiter.
27. Aged soap froth (reanalysed images taken from [1] and [6]; one of them did not yet reach the scaling state), dewetting network of PS films (analysed images taken from [32] and Reiter, G., unpublished) and of collagen films (two different samples, Fig.1c shows part of one of them).
28. James A. Glazier, S. P. Gross, and J. Stavans. Dynamics of two-dimensional soap froths. *Phys. Rev. A*, 36(1):306–12, 1987.
29. Same samples as in Fig.2. Additionally analysed are unpublished soap froth images by J. Glazier, PS images from [23] and images of other collagen samples.
30. J. Møller. Random Johnson–Mehl tessellations. *Adv. Appl. Prob.*, 24:814, 1992.
31. J. Møller. Topics in Voronoi and Johnson–Mehl tessellations. In *Proc. Séminaire Européen de Statistique*, Toulouse, 1996.
32. G. Reiter. Mobility of polymers in films thinner than their unperturbed size. *Europhys. Lett.*, 23(8):579–84, 1993.